Indian Journal of Pure & Applied Physics
Vol. 63, June 2025, pp. 508-516
DOI: 10.56042/ijpap.v63i6.16436

# Tailoring Elastic, Mechanical, Thermophysical and Ultrasonic Properties of TMCs (TM= V, Nb, Ta)

Praveen Singh[1*], Anurag Singh[1,2] & Devraj Singh[1]

[1]Department of Physics, Prof. Rajendra Singh (Rajju Bhaiya) Institute of Physical Sciences for Study and Research, Veer Bahadur Singh Purvanchal University, Jaunpur 222 003, India

[2]Department of Physics, Dr. Shyama Prasad Mukherjee Government Degree College, Bhadohi 221 401, India

*Received:4 March 2025; accepted:19 May 2025*

The elastic, mechanical, and thermoacoustic properties of transition metal carbides (VC, NbC, and TaC) were systematically analyzed with respect to orientation and temperature. The second-third-and fourth-order elastic constants were determined using the Coulomb and Born-Mayer potential model in the temperature regime 0–500 K. The analysis confirmed the elastic stability of VC, NbC and TaC. Mechanical properties derived from the second-order elastic constants, reveals that VC, NbC, and TaC exhibit brittle characteristics at room temperature. The thermal parameters, including Debye temperature, thermal conductivity and thermal relaxation time were evaluated along the <100>, <110>, <111> orientations. The Debye velocity and Debye temperature were observed to reach maximum values along the <100> direction. The relaxation time due to thermal phonon process is of the order of intermetallics. Ultrasonic attenuation was predominantly governed by the Akhiezer mechanism rather than thermal relaxation effects. The calculated values were compared with other B1-structured materials, and the performance of VC, NbC, and TaC was assessed based on the obtained parameters.

**Keywords:** Elastic properties, Mechanical behavior, Thermal properties, Ultrasonic attenuation

## 1 Introduction

Transition metal carbides (TMCs), such as vanadium carbide (VC), niobium carbide (NbC), and tantalum carbide (TaC) are of fundamental importance and represent a pivotal class of refractory materials in solid-state science and technology. These compounds possess a unique combination of high melting points, extreme hardness and exceptional resistance to wear and deformation under severe operating conditions, rendering them indispensable for high-performance engineering and industrial application[1]. The transition metal complex compounds possess some unique characteristics which is applicable for industrial applications like in aerospace, electronics, high temperature engineering, mechanical engineering, petroleum, chemical and nuclear industry[2-4]. Their electronic structures are studied by Schwarz[5], Zaoui *et al.*[6], Nakamura & Yashima[7]. The findings of the investigation[5-7] predicted that transition metal carbides have unusual properties due to mixture of ionic, covalent and metallic contributions to bonding. The exceptional mechanical and thermal performances of TMCs, existing in their original NaCl-type (B1 phase) crystal structure, have garnered significant attention, as in cutting tools, generators, magnetic storage devices, optoelectronic devices and maglev trains[8]. This has motivated researchers to extends applications of TMCs such as alternative electrocatalysts for Pt-group metal catalysts in renewable energy conversion reactions[9]. The lattice dynamics of transition of TMCs have been studied by Weber [10] and Isaev *et al.*[11]. Their findings support the covalent nature of TMCs. The cohesive properties and bonding mechanism of TMCs were also studied by Häglund *et al.*[12] by using linear muffin tin orbital method. In the other study, the thermophysical, electronic structure and bond nature of TMCs were studied with the use of the linearized method of "muffin-tin" orbitals (LMTO-ASA) by Zhukov *et al.*[13]. Li *et al.*[14] and Grossman *et al.*[15] calculated charge distribution and bulk modulus to predict hardness in TMCs by first principles method. Lu *et al.*[16] and Chauhan & Gupta[17] have calculated the thermodynamical parameters of carbides and nitrides cubic crystals with the help of Debye-Grüneisen model. Since the first principles calculations can predict the electronic properties of a wide class of transition metal compounds satisfactorily[18,19], but interionic potential models have also been found precise to elaborate the elastic properties and structural phase transition of TMCs[20-22]. However, in past few

*Corresponding author (E-mail: praveensingh379@gmail.com)

years successive progress was made for industrial and technological applications of these materials investigated by Cuppari *et al.*[23], Qin *et al.*[24] made remarkable progress in these rapidly developing field with particular focus on structure, property, synthesis and applicability of TMCs. Krutskii *et al*.[25] investigated TMCs, which are used as surfacing materials for the application of wear-resistant coatings to steel products. Various researchers also have been analyzed these transition metal compounds viz. Bhattacharya[26] investigated the effect of shock impact on some transition metal carbides and nitrides within the Debye-Grüneisen theory, Shang *et al*.[27] investigated the superconducting and topological properties of the rocksalt-type compounds NbC and TaC, Li *et al.*[28] studied, the interface bonding work, including interface bonding characteristics and electronic properties of α-Fe- and NaCl-type transition metal carbides using the first-principles calculation method. Due to unavailability of research on ultrasonic attenuation of TMCs motivated us to explore more about transition metal carbides using ultrasonic non-destructive techniques.

The paper aims to provide a comprehensive exploration of the elastic, mechanical, and thermophysical properties of VC, NbC, and TaC, emphasizing their crystallographic orientation and temperature dependencies. Employing the Coulomb and Born-Mayer potential models, this study calculates the SOECs, TOECs and FOECs, shedding light on their stability and deformation characteristics under diverse conditions. Moreover, ultrasonic properties are examined to elucidate the underlying mechanisms governing energy dissipation. By benchmarking these findings against other B1-structured TMCs, this work not only advances the fundamental understanding of TMCs but also paves the way for their optimization in applications demanding superior durability and performance under extreme conditions.

## 2 Theory

The stress-strain effect in crystals during wave propagation, is reported by SOECs[29], whereas TOECs displays the nonlinear strain features of the solids[30]. TOECs represents the anharmonic characteristics of the compounds, like Grüneisen variable and acoustic attenuation arising by thermal relaxation process and phonon viscosity mechanism between phonons etc.[31,32]. Fourth-order elastic constants, also known as FOECs, are parameters that describe the response of materials to large deformation and are important for understanding the anharmonic regime of materials and predicting their mechanical behavior under tension. They are related by the second derivative of the wave velocity with respect to the applied stress.[33,34] The potential utilized for the evaluation of these elastic constants is derived from the combination of Coulomb potential and Born-Mayer potential.

$$\mathcal{F}(r_o) = \mathcal{F}^C(r_o) + \mathcal{F}^B(r_o) \quad \ldots (1)$$

Here $\mathcal{F}^C(r_o)$ is the Coulomb/ electrostatic potential and $\mathcal{F}^B(r_o)$ is the Born Mayer repulsive Potential, given as

$$\mathcal{F}^C(r_o) = \pm\left(\frac{e^2}{r_0}\right) \text{ and } \mathcal{F}^B(r_o) = Aexp\left(\frac{-r_0}{b}\right) \quad \ldots (2)$$

In this context, the symbol (e) represents the fundamental electronic charge, while $(r_o)$ represent the nearest-neighbour distance, ($b$) denotes the hardness-parameter, and ($A$) signifies the strength-parameter[32]. In accordance with the lattice dynamics frameworks suggested by Leibfried and Ludwig[35], Ghate[36], Singh *et al.*[37] the lattice energy is temperature-dependent. Therefore, by integrating the vibrational-part with the static elastic constants SOECs, TOECs and FOECs ($C_{ij}$, $C_{ijk}$ and $C_{ijkl}$) can be derived as

$$C_{ij} = C_{ij}^0 + C_{ij}^{vib},\ C_{ijk} = C_{ijk}^0 + C_{ijk}^{vib} \text{ and } C_{ijkl} = C_{ijkl}^0 + C_{ijkl}^{vib} \quad \ldots (3)$$

In this context superscript (*0*) has been used to denote static portion at 0K and superscript (*vib*) has been used to denote the vibrational part of SOECs, TOECs and FOECs at a particular temperature. The expression for $C_{ij}$, $C_{ijk}$ and *Cijkl* are given in literature[37-39].

The SOECs are applied to enumerate the mechanical parameters like Young's modulus ($E$), bulk modulus ($B$), shear modulus ($G$), Tetragonal modulus ($Cs$), Poisson's ratio ($\nu$), Cauchy pressure, Zener anisotropic factor ($Z_A$) and Pugh's indicator ($B/G$)[37] and these parameters are placed in Table 1.

Within a cubic crystal, ultrasonic wave propagation entails three modes of ultrasonic velocities one

Table 1— The formulae for calculating the values of mechanical parameters

| | |
|---|---|
| $B = \frac{(C_{11}+2\,C_{12})}{3}$ | $G = \frac{(C_{11}-C_{12}+3C_{44})}{10} + \frac{2.5(C_{11}-C_{12})C_{44}}{4[C_{44}+3(C_{11}-C_{12})]}$ |
| $E = \frac{9GB}{G+3B}$ | $Cs = \frac{C_{11}-C_{12}}{2}$ |
| $Z_A = \frac{2C_{44}}{C_{11}-C_{12}}$ | $\nu = \frac{3B-2G}{6B+2G}$ |

longitudinal ($V_L$), one shear ($V_{S1}$) and one quasi shear ($V_{S2}$). The formulae for these velocities are given in literature[41]. The Debye average velocity as the average of longitudinal and shear velocity is given as

$$\frac{1}{{V_D}^3}=\left[\frac{1}{3}\left\{\frac{1}{{V_L}^3}+\frac{1}{{V_{S1}}^3}+\frac{1}{{V_{S2}}^3}\right\}\right]^{-\frac{1}{3}} \quad \ldots (4)$$

The Debye temperature is a substantial thermophysical parameter which interlinks elastic properties to thermal properties. The Debye temperature is computed via Debye velocity as[42]

$$T_D=\frac{h}{k_B}\left(\frac{3nN\rho}{4\pi m}\right)^{\frac{1}{3}}V_D \quad \ldots (5)$$

In this context, $V_D$ represents Debye average velocity, while $h$ denotes the Planck's constant. Additionally, $k_B$ signifies the Boltzmann's constant, and $n$ is the number of atoms in unit cell, m is molecular weight and $\rho$ is density of material.

The Debye temperature utilizes to evaluate thermal conductivity $\kappa$ as[40]

$$\kappa=\frac{AM\delta T_D^3 n^{1/3}}{\gamma^2 T} \quad \ldots (6)$$

In this context $\delta$ (in Å) is the cube root of volume per atom; The constant $A = 3.04\times10^{-8}$; $\gamma$ is defined as the Grüneisen parameter obtained with the help of SOECs and TOECs from Mason theory[43], $M$ = average atomic mass in amu. The relaxation time $\tau_{th}$ is the time in which thermal phonons restore its initial shape distorted by ultrasonic waves through conversion of acoustic to thermal energy is expressed as[40]

$$\tau_{th}=\frac{1}{2}\tau_L=\tau_S=\frac{3\kappa}{C_V V_D^2} \quad \ldots (7)$$

In this context, $\kappa$ represents thermal conductivity, while $C_V$ denotes the specific heat, calculated using data sourced from the AIP Handbook[44]. The acoustic coupling constant $D$, arising due to conversion of thermal to acoustical energy is expressed using following equation[40].

$$D = 9< (\gamma_i^j)^2> - \frac{3<\gamma_i^j>^2 \rho C_V T}{E_0} \quad \ldots (8)$$

The factors affecting ultrasonic attenuation in a perfect crystal are electron-phonon (e-p) interactions, phonon-phonon (p-p) interactions, and the thermoelastic relaxation mechanism. At room temperature, mean free paths of electrons and phonons do not coincide, leading to a disconnect between them. As temperatures rise, the influence of e-p interactions diminishes significantly. The key processes that predominantly impact ultrasonic attenuation at elevated temperatures are p-p interactions—often referred to as Akhiezer loss and thermoelastic relaxation[43].

The ultrasonic attenuation resulting from the thermoelastic-mechanism is determined by the following formula[40].

$$\left(\alpha/f^2\right)_{\text{th}}=\frac{4\pi^2<\gamma_i^j>^2 k\text{T}}{2\rho V_L^5} \quad \ldots (9)$$

The ultrasonic attenuation resulting from p-p interactions, applicable to both longitudinal and shear waves under defined conditions, is given as follows[37].

$$\left(\alpha/f^2\right)_{\text{L}}=\frac{4\pi^2\tau_{\text{th}}E_0\,(D_L/3)}{2\rho \text{V}_\text{L}^3} \quad \ldots (10)$$

$$\left(\alpha/f^2\right)_{\text{s}}=\frac{4\pi^2\tau_{th}E_0\,(\text{D}_S/3)}{2\rho V_S^3} \quad \ldots (11)$$

In this context $E_0$ represents the thermal energy density obtained from AIP hand book, while $V_L$ and $V_S$ denote the longitudinal and shear waves velocities.

## 3 Results and Discussion

The SOECs, TOECs and FOECs for TMCs over a temperature range of 0 to 500 K are evaluated with the help of lattice parameter and non-linearity parameters. The lattice parameters for VC, NbC and TaC are 2.08147 Å, 2.227215 Å, 2.2265 Å[7] respectively. The non-linearity parameter $b$ = 0.292 Å, 0.310 Å, 0.295 Å for the VC, NbC and TaC, respectively[45]. The obtained values of SOECs and TOECs are placed in Table 2 and Table 3, respectively.

The calculated SOECs $C_{11}$, $C_{12}$, $C_{44}$ are listed in Table 2 for comparison[6,10,46]. It is described in Table 2 that the $C_{11}$, $C_{12}$, and $C_{44}$ are similar with variation of 4% to 9% with listing values[6,10,46]. Table 2 and Table 3 clearly show that the magnitudes of SOECs and TOECs are minimum for NbC and maximum for VC.

It has been noted that compressibility parameter $C_{12}$ decreases with temperature while stiffness parameter $C_{11}$ and hardness parameter $C_{44}$ rises with temperature which predicts that chosen materials become stiffer and harder at higher temperature. The values of $C_{111}$, $C_{112}$, $C_{166}$ having negative magnitude depreciating with rising temperature and $C_{123}$ falling down with rising temperature and $C_{456}$ is constant because of the no contribution of the vibrational part.

Table 2 — Temperature dependent second-order elastic constants of TMCs (in $10^{11}$Nm$^{-2}$)

| Temp(K) | VC | | | NbC | | | TaC | | |
|---|---|---|---|---|---|---|---|---|---|
| | $C_{11}$ | $C_{12}$ | $C_{44}$ | $C_{11}$ | $C_{12}$ | $C_{44}$ | $C_{11}$ | $C_{12}$ | $C_{44}$ |
| 0 | 8.618 | 5.550 | 5.550 | 6.740 | 4.221 | 4.221 | 7.820 | 4.146 | 4.146 |
| | | | | 7.200[4] | 0.92[4] | 1.850[4] | 8.99[4] | 1.02[4] | 2.020[4] |
| | 5.00[10] | 2.90[10] | 1.50[10] | 6.20[10] | 2.00[10] | 1.50[10] | 5.50[10] | 1.50[10] | 1.90[10] |
| | | | | 6.27[46] | 1.59[46] | 1.51[46] | | | |
| 100 | 9.231 | 5.445 | 5.591 | 7.190 | 4.136 | 4.251 | 8.325 | 4.047 | 4.175 |
| 200 | 9.356 | 5.346 | 5.604 | 7.313 | 4.050 | 4.262 | 8.462 | 3.951 | 4.186 |
| 300 | 9.559 | 5.239 | 5.621 | 7.494 | 3.960 | 4.277 | 8.663 | 3.800 | 4.200 |
| 400 | 9.791 | 5.131 | 5.641 | 7.693 | 3.871 | 4.293 | 8.885 | 3.749 | 4.215 |
| 500 | 10.04 | 5.024 | 5.661 | 7.901 | 3.782 | 4.31 | 9.117 | 3.648 | 4.231 |

Table 3— Temperature dependent third-order elastic constants of TMCs (in $10^{11}$Nm$^{-2}$)

| Temp. (K) | Material | $C_{111}$ | $C_{112}$ | $C_{123}$ | $C_{144}$ | $C_{166}$ | $C_{456}$ |
|---|---|---|---|---|---|---|---|
| 0 | | -123.9 | -22.62 | 8.338 | 8.338 | -22.62 | 8.338 |
| | VC | -93.81[46] | -3.90[46] | 2.77[46] | 0.60[46] | | 2.13[46] |
| 100 | | -127.6 | -22.3 | 7.89 | 8.395 | -22.8 | 8.338 |
| 200 | | -127.7 | -22.06 | 7.441 | 8.439 | -22.83 | 8.338 |
| 300 | | -128.3 | -21.75 | 6.99 | 8.487 | -22.89 | 8.338 |
| 400 | | -129.1 | -21.44 | 6.54 | 8.537 | -22.95 | 8.338 |
| 500 | | -130 | -21.14 | 6.09 | 8.587 | -23.02 | 8.338 |
| 0 | | -97.32 | -17.22 | 6.36 | 6.36 | -17.22 | 6.36 |
| | | -91.14[46] | -5.78[46] | 5.41[46] | 1.05[46] | | 1.84[46] |
| 100 | | -99.99 | -16.96 | 5.985 | 6.405 | -17.35 | 6.36 |
| 200 | | -100.2 | -16.74 | 5.605 | 6.442 | -17.38 | 6.36 |
| 300 | NbC | -100.8 | -16.48 | 5.226 | 6.483 | -17.43 | 6.36 |
| 400 | | -101.5 | -16.2 | 4.847 | 6.523 | -17.48 | 6.36 |
| 500 | | -102.3 | -15.96 | 4.468 | 6.564 | -17.54 | 6.36 |
| 0 | | -115.8 | -16.97 | 6.369 | 6.369 | -16.97 | 6.369 |
| 100 | | -119 | -16.65 | 5.912 | 6.413 | -17.1 | 6.369 |
| 200 | TaC | -119.2 | -16.38 | 5.455 | 6.451 | -17.13 | 6.369 |
| 300 | | -119.9 | -16.08 | 4.997 | 6.492 | -17.18 | 6.369 |
| 400 | | -120.7 | -15.77 | 4.539 | 6.533 | -17.23 | 6.369 |
| 500 | | -121.6 | -15.46 | 4.081 | 6.574 | -17.29 | 6.369 |

Among TOECs maximum variation is visualized in $C_{123}$ with respect to temperature. These results have been compared with available literature[46]. From Table 2, the Cauchy's relation[47] $C_{12}^0 = C_{14}^0$, $C_{112}^0 = C_{166}^0$, $C_{123}^0 = C_{144}^0 = C_{456}^0$ are obeyed. Cauchy's criterion is not obeyed at other temperatures as interionic stress is more ionic. The criterion[48] of elastic stability ($C_{11} - C_{12} > 0$, $C_{44} > 0$, $C_{11} + 2C_{12} > 0$) has been satisfied for TMCs which shows that TMCs are mechanically stable. The values of FOECs for the selected TMCs are presented in Table 4.

From Table 4, $C_{1111}$ values for VC, NbC, TaC are highest and have positive coefficient and have magnitudes greater than SOECs and TOECs. The coefficients of the other FOECs are either negative or positive and their values are lower than the $C_{1111}$. It is depicted from Table 4, $C_{1456}$ remain unchanged due to negligible contribution of vibrational energy. No literature is available for TMCs to compare fourth order elastic constants that's why it is compared with similar $B_1$ type materials like copper[49] and platinum group metal nitrides[39] values are in good agreement.

The mechanical properties are computed applying second-order elastic constants at 0K and 300K for the TMCs and obtained values are compared in Table 5 with the available values[18,20,46].

The maximum bulk modulus is for VC and minimum for NbC as shown in Table 5, since values of $C_{11}$ and $C_{12}$ of VC are higher than those of NbC and TaC. This predicts that VC is tough and NbC is the fragile. The higher bulk modulus for VC depicts that VC is less compressible with respect to NbC and TaC. The higher $G$ values for VC inference that toughness of VC is higher than NbC and TaC. The Pugh's index ($B/G$), a comparison of fracture to toughness measures the brittleness and ductility of materials. If ($B/G$) is greater than 1.75 then material is ductile otherwise brittle. From Table 5 it is clear that

Table 4 — Temperature dependent fourth-order elastic constants of TMCs (in $10^{11}$Nm$^{-2}$)

| | TMCs | 0K | 100K | 200K | 300K | 400K | 500K |
|---|---|---|---|---|---|---|---|
| $C_{1111}$ | VC | 157.3 | 161.5 | 161.6 | 162.2 | 163 | 163.9 |
| | NbC | 123.9 | 127 | 127.2 | 127.7 | 128.4 | 129.3 |
| | TaC | 151 | 154.5 | 154.5 | 155.1 | 155.8 | 156.7 |
| $C_{1112}$ | VC | 10.63 | 10.68 | 10.8 | 10.87 | 10.95 | 11.02 |
| | NbC | 8.105 | 8.161 | 8.247 | 8.31 | 8.371 | 8.432 |
| | TaC | 8.076 | 8.142 | 8.257 | 8.341 | 8.422 | 8.504 |
| $C_{1122}$ | VC | 12.08 | 11.9 | 11.76 | 11.59 | 11.42 | 11.24 |
| | NbC | 9.215 | 9.068 | 8.939 | 8.79 | 8.641 | 8.493 |
| | TaC | 9.187 | 8.988 | 8.824 | 8.634 | 8.442 | 8.251 |
| $C_{1123}$ | VC | -1.948 | -1.916 | -1.887 | -1.855 | -1.823 | -1.792 |
| | NbC | -1.486 | -1.46 | -1.434 | -1.407 | -1.38 | -1.353 |
| | TaC | -1.488 | -1.454 | -1.421 | -1.387 | -1.352 | -1.319 |
| $C_{1144}$ | VC | -1.948 | -1.965 | -1.975 | -1.987 | -1.999 | -2.012 |
| | NbC | -1.486 | -1.499 | -1.508 | -1.518 | -1.528 | -1.539 |
| | TaC | -1.488 | -1.502 | -1.511 | -1.522 | -1.534 | -1.545 |
| $C_{1155}$ | VC | 10.63 | 10.7 | 10.69 | 10.69 | 10.69 | 10.69 |
| | NbC | 8.105 | 8.15 | 8.145 | 8.145 | 8.148 | 8.152 |
| | TaC | 8.076 | 8.126 | 8.116 | 8.115 | 8.117 | 8.121 |
| $C_{1255}$ | VC | -1.948 | -1.96 | -1.965 | -1.972 | -1.98 | -1.988 |
| | NbC | -1.486 | -1.495 | -1.499 | -1.506 | -1.512 | -1.518 |
| | TaC | -1.488 | -1.497 | -1.501 | -1.508 | -1.514 | -1.52 |
| $C_{1266}$ | VC | 12.08 | 12.19 | 12.21 | 12.24 | 12.28 | 12.32 |
| | NbC | 9.215 | 9.295 | 9.312 | 9.34 | 9.371 | 9.404 |
| | TaC | 9.187 | 9.271 | 9.289 | 9.318 | 9.35 | 9.385 |
| $C_{1456}$ | VC | -1.948 | -1.948 | -1.948 | -1.948 | -1.948 | -1.948 |
| | NbC | -1.486 | -1.486 | -1.486 | -1.486 | -1.486 | -1.486 |
| | TaC | -1.488 | -1.488 | -1.488 | -1.488 | -1.488 | -1.488 |
| $C_{4444}$ | VC | 12.08 | 12.23 | 12.28 | 12.34 | 12.41 | 12.48 |
| | NbC | 9.215 | 9.325 | 9.365 | 9.418 | 9.475 | 9.534 |
| | TaC | 9.187 | 9.302 | 9.345 | 9.401 | 9.461 | 9.523 |
| $C_{4455}$ | VC | -1.948 | -1.95 | -1.952 | -1.954 | -1.956 | -1.958 |
| | NbC | -1.486 | -1.488 | -1.489 | -1.491 | -1.492 | -1.494 |
| | TaC | -1.488 | -1.49 | -1.491 | -1.492 | -1.494 | -1.495 |

Table 5 — $E$, $B$, $G$, $C_S$ (all in $10^{11}$N/m$^2$), $B/G$, $Z_A$ and $\nu$ of TMCs at 0K and 300K

| TMCs | Temp.[K] | $E$ | $B$ | $G$ | $Cs$ | $B/G$ | $Z_A$ | $\nu$ |
|---|---|---|---|---|---|---|---|---|
| VC | 0 | 8.541 | 6.573<br>3.58[20] | 3.327 | 1.534 | 1.975 | 3.619 | 0.2834 |
| | 300 | 9.649 | 6.679 | 3.831 | 2.160 | 1.743 | 2.602 | 0.2592 |
| NbC | 0 | 6.672<br>5.480[18]<br>6.165[46] | 5.061<br>3.020[18]<br>2.880[46]<br>3.600[20] | 2.606<br>2.290[18]<br>1.731[46] | 1.259<br>3.140[18] | 1.942<br>132.0[18] | 3.352<br>0.32[46] | 0.2803<br>0.197[18]<br>0.160[46] |
| | 300 | 7.534 | 5.138 | 3.000 | 1.767 | 1.713 | 2.421 | 0.2556 |
| TaC | 0 | 7.568<br>6.427[18]<br>6.547[46] | 5.371<br>3.680[18]<br>3.180[46]<br>4.010[20] | 2.991<br>2.670[18]<br>1.896[46] | 1.837<br>3.990[18] | 1.796<br>1.38[18] | 2.257<br>0.44[46] | 0.2652<br>0.208[18]<br>0.154[46] |
| | 300 | 8.361 | 5.454 | 3.359 | 2.406 | 1.624 | 1.745 | 0.2445 |

fracture to toughness ratio ($B/G$) is greater than 1.75 at absolute zero while it is smaller than 1.75 at room temperature. This illustrates that chosen transition metal carbides are ductile at absolute zero and brittle at room temperature. The ν values are greater than 0.2 but less than 0.5, which demonstrates that the intrinsic forces are non-central in character for the TMCs. The identity $\nu$=0.25 for ionic material is satisfied in present case which demonstrates that the chosen carbides are of ionic character. The Cauchy's pressure

($C_{12}$ - $C_{44}$) and Poisson ratio ($v$) can also be evaluated to determine ductility and brittleness of the material. If ($C_{12}$ - $C_{44}$) >0 and $v$ >0.3, the material is ductile and if ($C_{12}$ - $C_{44}$) <0 and $v$ <0.3, the substance is of brittle character[50]. It is depicted from Table 2 that ($C_{12}$ - $C_{44}$) <0 and $v$ < 0.3 at room temperature, which predicts brittleness of TMCs and validates previous prediction of brittleness based on Pugh's ratio. One of the anisotropy parameter i.e., Zener index ($Z_A$) is unity for isotropic crystals but for $Z_A \neq 1$ the material is anisotropy in nature. In present case the estimated values of $Z_A$ suggest that chosen TMCs are anisotropic in nature. The density and SOECs are utilized to calculate the longitudinal and shear modes of ultrasonic non-linear velocities in <100>, <110>, and <111> orientations. The obtained values of $V_L$, $V_{S1}$, and $V_{S2}$ have been presented in Table 6 for TMCs.

Table 6 — Orientation dependent $V_L$, $V_{S1}$, and $V_{S2}$ (in $10^3$m/s) for TMCs in 100-500K

| TMCs | Orientation | Temp. (K) | $V_L$ | $V_{S1}$ | $V_{S2}$ | $V_D$ |
|---|---|---|---|---|---|---|
| | <100> | 100 | 3.991 | 3.106 | 3.106 | 3.313 |
| | <100> | 200 | 4.018 | 3.109 | 3.109 | 3.321 |
| | <100> | 300 | 4.061 | 3.114 | 3.114 | 3.331 |
| | <100> | 400 | 4.110 | 3.120 | 3.120 | 3.343 |
| | <100> | 500 | 4.161 | 3.125 | 3.125 | 3.356 |
| | <110> | 100 | 4.723 | 3.106 | 2.556 | 3.079 |
| | <110> | 200 | 4.728 | 3.109 | 2.630 | 3.132 |
| VC | <110> | 300 | 4.740 | 3.114 | 2.730 | 3.199 |
| | <110> | 400 | 4.755 | 3.120 | 2.835 | 3.266 |
| | <110> | 500 | 4.771 | 3.125 | 2.941 | 3.329 |
| | <111> | 100 | 4.943 | 2.322 | 2.322 | 2.614 |
| | <111> | 200 | 4.942 | 2.351 | 2.351 | 2.645 |
| | <111> | 300 | 4.945 | 2.391 | 2.391 | 2.688 |
| | <111> | 400 | 4.951 | 2.434 | 2.434 | 2.733 |
| | <111> | 500 | 4.957 | 2.478 | 2.478 | 2.779 |
| | <100> | 100 | 3.020 | 2.322 | 2.322 | 2.483 |
| | <100> | 200 | 3.046 | 2.325 | 2.325 | 2.489 |
| | <100> | 300 | 3.083 | 2.329 | 2.329 | 2.498 |
| | <100> | 400 | 3.124 | 2.333 | 2.333 | 2.508 |
| | <100> | 500 | 3.165 | 2.338 | 2.338 | 2.517 |
| | <110> | 100 | 3.546 | 2.322 | 1.968 | 2.342 |
| | <110> | 200 | 3.551 | 2.325 | 2.034 | 2.387 |
| NbC | <110> | 300 | 3.562 | 2.329 | 2.117 | 2.439 |
| | <110> | 400 | 3.575 | 2.333 | 2.202 | 2.490 |
| | <110> | 500 | 3.588 | 2.338 | 2.285 | 2.537 |
| | <111> | 100 | 3.705 | 1.757 | 1.757 | 1.977 |
| | <111> | 200 | 3.705 | 1.784 | 1.784 | 2.005 |
| | <111> | 300 | 3.708 | 1.817 | 1.817 | 2.041 |
| | <111> | 400 | 3.713 | 1.852 | 1.852 | 2.078 |
| | <111> | 500 | 3.718 | 1.888 | 1.888 | 2.116 |
| | <100> | 100 | 2.395 | 1.696 | 1.696 | 1.839 |
| | <100> | 200 | 2.415 | 1.698 | 1.698 | 1.843 |
| | <100> | 300 | 2.443 | 1.701 | 1.701 | 1.849 |
| | <100> | 400 | 2.474 | 1.704 | 1.704 | 1.855 |
| | <100> | 500 | 2.507 | 1.708 | 1.708 | 1.861 |
| | <110> | 100 | 2.672 | 1.696 | 1.717 | 1.875 |
| | <110> | 200 | 2.676 | 1.698 | 1.763 | 1.898 |
| TaC | <110> | 300 | 2.684 | 1.701 | 1.821 | 1.925 |
| | <110> | 400 | 2.694 | 1.704 | 1.881 | 1.952 |
| | <110> | 500 | 2.704 | 1.708 | 1.941 | 1.977 |
| | <111> | 100 | 2.758 | 1.393 | 1.393 | 1.562 |
| | <111> | 200 | 2.758 | 1.413 | 1.413 | 3.313 |
| | <111> | 300 | 2.760 | 1.439 | 1.439 | 3.321 |
| | <111> | 400 | 2.763 | 1.466 | 1.466 | 3.331 |
| | <111> | 500 | 2.767 | 1.493 | 1.493 | 3.343 |

Equation (4) is applied to measure the Debye average velocities in different directions and are presented in Table 6.

From Table 6, it is visualized that $V_L$ is maximum in the <111> direction while minimum in <100> direction in temperature range 100-500K. The lattice

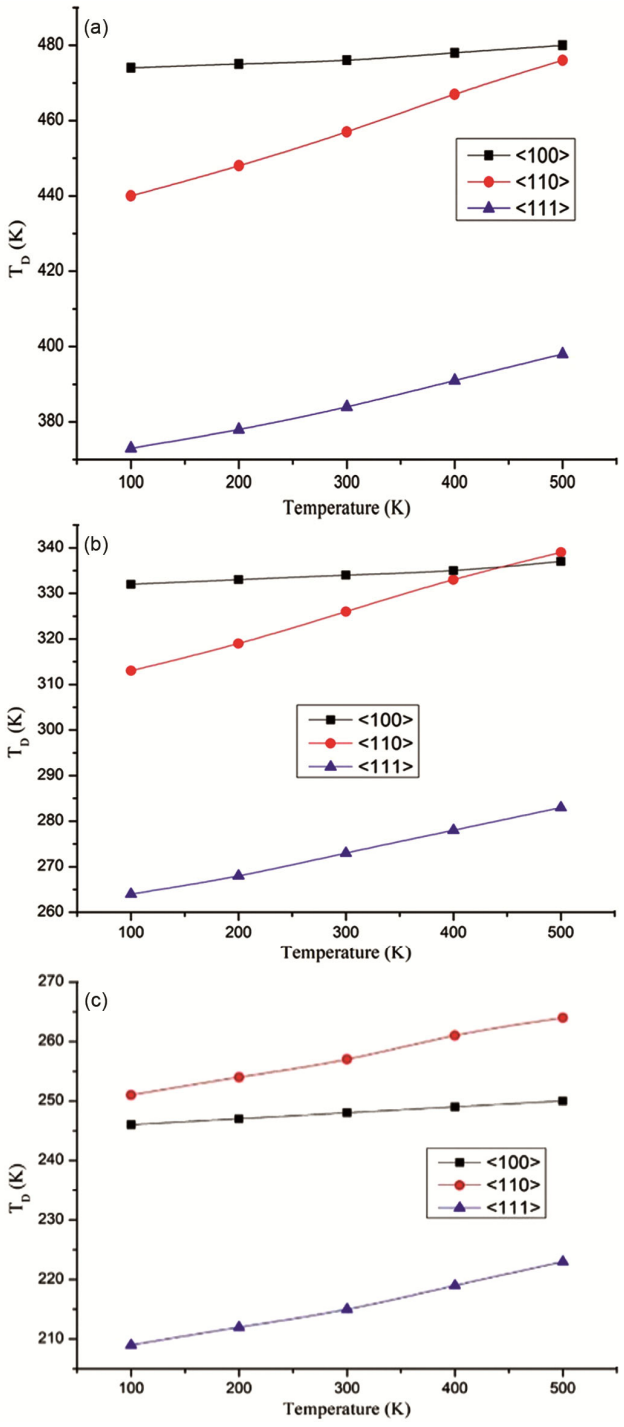


Fig. 1— Temperature and direction dependent Debye temperature ($T_D$) for (a) VC, (b) NbC, and (c) TaC

vibrations in compressional mode dominate over transverse mode due to dominance of longitudinal velocities over shear velocities. The velocity is inversely related to the density by virtue of which the non-linear acoustic velocity decreases as VC < NbC< TaC, as shown in Table 6. The ultrasonic velocities are directly proportional to SOECs which are proportional to temperature. Hence ultrasonic velocities are increasing with temperature. The Debye temperature $T_D$ plays an important role to establish connection between elastic and thermal characteristics of materials. The Debye velocity is accomplished to enumerate one of the very important thermodynamical parameters *i.e.,* Debye temperature ($T_D$) by means of Eq (5) and is shown in Fig. 1.

The $T_D$ decreases from VC to TaC because Debye temperature is inversely related to molar mass which is of the order of the values in existing literature[21]. The obtained data of the acoustic coupling constant ($D_L$, $D_{S1}$, $D_{S2}$), thermal conductivity ($\kappa$), thermal relaxation time ($\tau$) and ultrasonic attenuation ($\alpha/f^2$) are figured out in Table 7.

From Table 7, the thermal conductivity follows the order VC >NbC >TaC because thermal conductivity is directly proportional to Debye temperature ($T_D$). The thermal conductivities for chosen transition metal carbides are maximum in <100> orientation like Debye temperature. This clearly indicates that VC, NbC and TaC have better thermal properties along <100> direction. Table 7 depicts that value of $D$ decreases from VC to TaC. The thermal relaxation time is the time in which phonon regains its original equilibrium condition which was distorted due to thermal disturbances of wave propagation. The values of thermal relaxation time are found to be $10^{-11}$s in present case which is comparable with[50]. The order of $\tau_{th}$ confirms that chosen VC, NbC, and TaC are intermetallics. The acoustic wave attenuation has been computed using Eqs. (10) and (11) at temperature 300K in <100>, <110> and <111> orientations for the chosen TMCs.

The obtained results of $(\alpha/f^2)_{th}$, $(\alpha/f^2)_{l}$, $(\alpha/f^2)_{S1}$ and $(\alpha/f^2)_{S2}$ for TMCs are presented in Table 7. Table 7 demonstrates that thermoelastic attenuation is very much small in comparison to phonon viscosity mechanism (Akhiezer loss). The nonlinear ultrasonic attenuation increases with rising temperature in <100>, <110> and <111> orientations for TMCs. The behaviour of $(\alpha/f^2)$ is very close to platinum group metal carbides[39]. Total attenuation as the sum of

Table 7 — $\kappa$ ($Wm^{-1}K^{-1}$), $\tau$ ($10^{-11}$s), $(\alpha/f^2)_{th}$, $(\alpha/f^2)_{Akh(l)}$, $(\alpha/f^2)_{Akh(S1)}$, $(\alpha/f^2)_{Akh(S2)}$ of TMCs (all in $10^{-18}$ $Nps^2m^{-1}$) at T=300K

| Material | Direction | $\kappa$ | $D_L$ | $D_{S1}$ | $D_{S2}$ | $\tau$ | $(\alpha/f^2)_{th}$ | $(\alpha/f^2)_{Akh(L)}$ | $(\alpha/f^2)_{Akh(S1)}$ | $(\alpha/f^2)_{Akh(S2)}$ |
|---|---|---|---|---|---|---|---|---|---|---|
| | <100> | 15.27 | 14.04 | 1.62 | 1.62 | 2.03 | 1.07 | 35.15 | 4.49 | 4.49 |
| VC | <110> | 4.53 | 20.54 | 1.97 | 18.07 | 0.65 | 0.44 | 10.51 | 1.78 | 24.20 |
| | <111> | 2.06 | 19.93 | 10.96 | 10.96 | 0.41 | 0.21 | 6.27 | 15.25 | 15.25 |
| | <100> | 9.93 | 13.70 | 1.52 | 1.52 | 2.72 | 1.91 | 75.95 | 9.79 | 9.79 |
| NbC | <110> | 3.03 | 19.62 | 1.88 | 18.34 | 0.86 | 0.87 | 23.23 | 3.97 | 51.72 |
| | <111> | 1.37 | 19.11 | 11.10 | 11.10 | 0.55 | 0.41 | 13.53 | 33.39 | 33.39 |
| | <100> | 8.04 | 13.36 | 1.24 | 1.24 | 3.87 | 2.48 | 131.87 | 18.08 | 18.08 |
| TaC | <110> | 2.77 | 17.58 | 1.52 | 1.52 | 1.24 | 1.75 | 41.22 | 6.99 | 77.20 |
| | <111> | 1.28 | 17.44 | 12.30 | 12.30 | 0.87 | 0.89 | 25.89 | 64.44 | 64.44 |

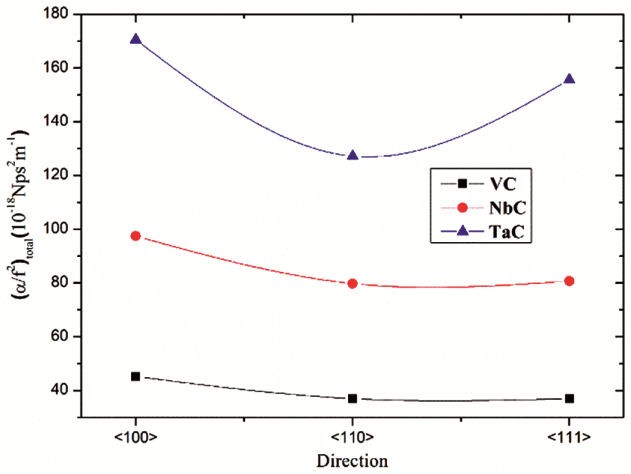


Fig. 2—Net acoustic attenuation of TMCs in different directions at room temperature

thermal and Akhiezer attenuation for the chosen TMCs have been plotted in Fig. 2 for TMCs at the temperature 300K along <100>, <110> and <111> directions.

Figure 2 depicts that total attenuation for TMCs largest in <100> and smallest in <111> orientations. From Fig. 2 it is evident that total attenuation is maximum for TaC and minimum for VC. The ultrasonic attenuation follows the order for the chosen substance as VC< NbC<TaC. From Table 7 it is visualized that ultrasonic attenuation follows the order TaC > NbC > VC which inference that ultrasonic attenuation is directly proportional to molecular weight[49]. It is evident that total attenuation is lowest in <110> orientation and highest for <100> orientation. It seems that VC is suitable material for industrial use in <110> direction because of minimum attenuation.

## 4 Conclusion

The Born model has been applied to enumerate the SOECs, TOECs and FOECs and validated successfully. The validation of Born stability criteria indicates the elastic stability of TMCs. Pugh's index shows the brittle nature of the chosen materials at room temperature. Cauchy criteria for SOECs hold valid at 0K, and failed at temperatures above 0K for selected group V transition metal carbides. The better thermodynamic behaviour of the VC, NbC, and TaC have been found along <100> direction. The thermal relaxation time is of the order of $10^{-11}$s, which predicts intermetallic nature of TMCs. The lowest attenuation magnitude for VC predicts that VC will be utilized industrial applications with respect to NbC and TaC. The <110> direction has lowest ultrasonic attenuation values for TMCs, thus <110> direction is preferred for industrial application.

## Acknowledgements

Authors thank the Department of Science and Technology, New Delhi for providing support under DST-PURSE scheme (SR/PURSE/2024/230) to V.B.S. Purvanchal University, Jaunpur, Uttar Pradesh, India. We also appreciate the editor and the reviewers for their precious time in reviewing our manuscript and providing valuable comments.

## References

1 Wells A F, *Structural Inorganic Chemistry*, 5th ed, Claredon Press Oxford (1984).
2 Shveikin G P, Alyamovskii S I, Zainulin Y G, Gusev A I, Gubanov V A & Kurmaev E Z, *Russian Chem Rev*, 55 (1986) 1175.
3 de Novion C H & Landesman J P, *Pure Appl Chem*, 57 (1985) 1391.
4 Gusev A I, Rempel A A & Magerl A J, Disorder and Order in Strongly Nonstoichiometric Compounds: Transition Metal Carbides, Nitrides and Oxides (Springer Berlin, Heidelberg), 1st Edn, 2021.
5 Schwarz K, *Crit Rev Solid State Mater Sci*, 13 (1987) 211.
6 Zaoui A, Bouhafs B & Ruterana P, *Mater Chem Phys*, 91 (2005) 108.
7 Nakamura K & Yashima M, *Mater Sci Eng B*, 148 (2008) 69.
8 Ham D J & Lee J S, *Energies*, 2 (2009) 873.

9 Joo S H & Lee J S, *J Catal*, 404 (2021) 911.
10 Weber W, *Phys Rev B*, 8 (1973) 5082.
11 Isaev E I, Simak S I, Abrikosov I A, Ahuja R, Vekilov Y K & Johansson B, *J Appl Phys*, 101 (2007) 123519.
12 Häglund J, Grimvall G, Jarlborg T & Guillermet A F, *Phys Rev B*, 43 (1991) 14400.
13 Zhukov V P, Gubanov V A & Jarlborg T, *J Phys Chem Solids*, 46 (1985) 1111.
14 Li C B, Li M K, Liu F Q & Fan X J, *Mod Phys Lett B*, 18 (2004) 281.
15 Grossman J C, Mizel A, Côté M, Cohen M L & Louie S G, *Phys Rev B*, 60 (1999) 6343.
16 Lu XG, Selleby M & Sundman B, *Acta Mater*, 55 (2007) 1215.
17 Chauhan M & Gupta D C, *Phase Transit*, 88 (2015) 1193.
18 Srivastava A, Chauhan M & Singh R K, *Phase Transit*, 84 (2011) 58.
19 Liu Y, Jiang Y, Zhou R & Feng J, *J Alloys*, 582 (2014) 500.
20 Singh A, Aynyas M & Sanyal S P, *Phase Transit*, 82 (2009) 576.
21 Srivastava A & Diwan B D, *Can J Phys*, 90 (2012) 338.
22 Varshney D, Shriya S & Singh N, *AIP Conf Proc*, 1512 (2013) 1016,
23 Cuppari M & Santos S, *Metals*, 6 (2016) 250.
24 Qin T, Wang Z, Wang Y, Besenbacher F, Otyepka M & Dong M, *Nano-Micro Lett*, 13 (2021) 183.
25 Krutskii Y L, Gudyma T S, Kuchumova I D, Khabirov R R & Antropova K A, *Izv Ferr Metall*. 65 (2022) 305.
26 Bhattacharya C, *Comput Mater Sci*, 127 (2017) 85.
27 Shang T, Zhao J Z, Gawryluk D J, Shi M, Medarde M & Shiroka T, *Phys Rev B*, 101 (2020) 214518.
28 Li J, Xu Y & Li W, *Materials*,16 (2023) 1887.
29 Born M & Huang K, Dynamical Theory of Crystal Lattices, Oxford Academic, New York (1996).
30 Wallace D C, *Solid State Phys*, 25 (1970) 301.
31 Yang X, Meng Z & Cao H, *Adv Mater Sci Eng*, 2021 (2021) 8726250.
32 Brugger K, *Phys Rev*,133 (1964) A1611.
33 Markenscoff X, *J Phys Colloq*, 40 (C8) (1979) 213.
34 Pandit A & Bongiorno A, *Comput Phys Commun*, 288 (2023), 108751.
35 Leibfried G & Ludwig W, 'Theory of Anharmonic Effects in Crystals' in Solid State Physics, edited by F Seitz & D Turnbull (Academic Press, New York), 12 (1961) 275.
36 Ghate P B, *Phys Rev*, 139 (1965) A1666.
37 Singh A, Kumar A, Singh D, Thakur R K & Maddheshiya A K, *Indian J Pure Appl Phys*, 62 (2024) 834.
38 Bala J, Singh S P, Verma A K, Singh D K & Singh D, *Indian J Phys*, 96 (2022) 3191.
39 Kumar R, Singh D, Tripathi S, Khenata R & Bin-Omram S, *Johnson Matthey Technol Rev*, 69(3) (2025) 437.
40 Chauhan J, Singh D, Khenata R, Meradji H, Bin-Omran S & Maddheshiya A K, *Z. Naturforsch A*, 80 (2025) 233.
41 Singh A & Singh D, *Z. Naturforsch A*, 78 (2023) 947.
42 Jasiukiewicz C & Karpus V, *Solid State Commun*, 128 (2003) 167.
43 Mason W P, 'Effect of impurities phonons process on the ultrasonic attenuation of germanium crystal quartz and silicon' in Physical Acoustics: Principle and methods, Vol. III B, edited by W P Mason (Academic press, New York), 1965, p. 277.
44 Gray D E, American Institute of Physics Handbook (McGraw-Hill, New York), 3rd Edn, (1972).
45 Tosi M P & Fumi F G, *J Phys Chem Solids,* 25 (1964) 45.
46 Ahmed R, Mahamudujjaman M, Afzal M A, Islam M S, Islam R S & Naqib S H, *J Mater Res Technol,* 24 (2023) 4808.
47 Liao M, Liu Y, Lai Z & Zhu J, *Ceram Int*, 47 (2021) 27535.
48 Cousins C S G, *J Phys C Solid State Phys*, 4 (1971) 1117.
49 Soma H & Hiki Y, *J Phys Soc Jpn*, 37 (1974) 544.
50 Singh A, Tripathi S & Singh D, *Mod Phys Lett B*, 38 (2024) 2450280.